ELSEVIER

Journal of Biomechanics 41 (2008) 668–676

JOURNAL OF BIOMECHANICS

www.elsevier.com/locate/jbiomech
www.JBiomech.com

Analysis of musculoskeletal loading in an index finger during tapping

John Z. Wu[a,*], Kai-Nan An[b], Robert G. Cutlip[a], Kristine Krajnak[a], Daniel Welcome[a], Ren G. Dong[a]

[a]National Institute for Occupational Safety and Health, NIOSH/CDC, 1095 Willowdale Road, MS-2027, Morgantown, WV 26505, USA
[b]Mayo Clinic College of Medicine, Rochester, MN 55905, USA

Accepted 25 September 2007

Abstract

Since musculoskeletal disorders of the upper extremities are believed to be associated with repetitive excessive muscle force production in the hands, understanding the time-dependent muscle forces during key tapping is essential for exploring the mechanisms of disease initiation and development. In the current study, we have simulated the time-dependent dynamic loading in the muscle/tendons in an index finger during tapping. The index finger model is developed using a commercial software package AnyBody, and it contains seven muscle/tendons that connect the three phalangeal finger sections. Our simulations indicate that the ratios of the maximal forces in flexor digitorum superficialis (FS) and flexor digitorum profundus (FP) tendons to the maximal force at the fingertip are 0.95 and 2.9, respectively, which agree well with recently published experimental data. The time sequence of the finger muscle activation predicted in the current study is consistent with the EMG data in the literature. The proposed model will be useful for bioengineers and ergonomic designers to improve keyboard design minimizing musculoskeletal loadings in the fingers.
Published by Elsevier Ltd.

Keywords: Index finger; Muscle force; Muscle–tendon excursion; Tapping; Simulations

1. Introduction

In the last 10 years, computer use has become prevalent both in the workplace and at home. According to the U.S. Census Bureau, 56.1% of employed adults use computers at work. In addition, 61.8% of U.S. households have computers, and in those households, 66.1% of adults and 82.6% of children (age 3–18) use computers (Day et al., 2005). Epidemiological studies have demonstrated that excessive computer use could result in an increased risk of developing musculoskeletal disorders (MSDs) of the upper extremities (e.g., Cail and Aptel, 2003; Faucett and Rempel, 1996; Gerr et al., 2006; Hales et al., 1994; Marcus and Gerr, 1996). For example, a prospective study examining the effects of occupational computer use in workers over a 3 year period demonstrated that workers using computers for at least 15 h each week were at an increased risk for developing neck/shoulder and hand/arm symptoms and disorders (Gerr et al., 2006). The primary injuries to the hands and arms were tendonitis of the extensor tendons and the digital flexor tendons.

Electromyography (EMG) studies evaluating muscle activity during typing suggest that MSDs in the upper extremities are related to excessive repetitive musculoskeletal loading. For example, Gerard et al. (1999) have examined EMG activity to evaluate the effects of typing force and keypad stiffness on MSDs and Woods and Babski-Reeves (2005) analyzed the EMG of the hand–arm to determine the effects of posture on MSDs. The relationships among tendon force, contact force at the fingertip, and finger posture have been investigated by using a force transducer mounted directly onto the flexor digitorum superficialis (FS) and flexor digitorum profundus (FD) tendons of the fingers (Schuind et al., 1992; Dennerlein et al., 1999; Kursa et al., 2005). The reported ratio of the force in the FS tendon to the contact force at the fingertip varied from 1.5 ± 1.0 (Kursa et al., 2005) and 1.7 ± 1.5 (Schuind et al., 1992) to 3.3 ± 1.4 (Dennerlein et al., 1999). The reported ratio of the FP tendon force to

*Corresponding author. Tel.: +1 304 285 5832; fax: +1 304 285 6265.
E-mail address: jwu@cdc.gov (J.Z. Wu).

0021-9290/$ - see front matter Published by Elsevier Ltd.
doi:10.1016/j.jbiomech.2007.09.025

the fingertip force showed more variance, from 2.4 ± 0.7 (Kursa et al., 2005) to 7.9 ± 6.3 (Schuind et al., 1992). Dennerlein et al. (1998) compared the experimentally measured tendon force with that calculated using an inverse dynamic approach and found that the measured tendon force is consistently greater than that predicted by the model with the muscle in an isometric contraction. The dynamic force distribution in the finger muscles during tapping has not been investigated either experimentally or theoretically.

Because the experimental evaluation of the dynamic loading in individual muscles of the hand during typing is technically difficult, researchers have studied the dynamic contact force between the fingertip and keypad, and joint angle motions, and assumed that these indices are related to the muscle/tendon excursions (e.g., Gerard et al., 1999; Nelson et al., 2000). The most extensive analyses were performed by Jindrich et al. (2004) who analyzed joint torques and kinematic energy of the finger sections during tapping. Dennerlein et al. (1998) assessed muscle activities during the keystroke task; their results suggested that the role of the extrinsic finger flexors during a keystroke is to overcome the activation force of the keyswitch, while the extrinsic extensors are to perform the upswing rather than stop the downswing. Kuo et al. (2006) analyzed the relationship among joint coordination, kinematics, muscle activation patterns, and energy profiles during the tapping task and found that the activation of the intrinsic muscles began slightly before the initiation of the downswing motion, while the activation of the extrinsic flexors started after the initiation of the downward finger motion. However, a quantitative analysis of the dynamic loading in each individual muscle and tendon in a finger has not been performed during the tapping test.

One of the most promising theoretical approaches for exploring the muscle forces in fingers during typing is a multi-body biomechanical model. In such models, a finger is modeled as bony sections that are connected with muscles and tendons. Multiple biomechanical models of the hands and fingers have been developed to simulate different scenarios. For example, Sancho-Bru et al. (2001, 2003) developed a whole hand model simulating the muscle loading for static gripping and free movements; Brook et al. (1995) developed a biomechanical model of the dynamics of the index finger and applied their model to simulate the muscle forces in pinch grip and disc rotation; Biggs and Horch (1999) proposed a 3D kinematic long-finger model and validated their model via the experimental data of tendon/muscle excursions. All these mathematical hand models were formulated analytically and rely on certain simplifying assumptions. The most "realistic" biomechanical finger models were proposed by Valero-Cuevas et al. (2003, 2005), who included anatomically realistic tendon/muscle network connections into their models.

The goal of the current study is to analyze the dynamic muscle forces in an index finger during tapping using a universal finger model developed on a platform of the commercial software package AnyBody (AnyBody Technology Inc., Aalborg, Denmark). Specifically, we are going to theoretically analyze the joint torques and muscle forces and their relationships to the impact force at the fingertip and the mass moment of inertia of the finger sections. Furthermore, the theoretically predicted muscle force variations in the finger will be compared with the EMG signals of the previous study (Kuo et al., 2006). The proposed model will be applicable for realistic problems and it will include realistic bony shapes, nonlinear mechanical properties of the ligaments and tendons and physiological muscle models.

2. Methods

2.1. Index finger model

The finger model was developed on the platform of the commercial software package AnyBody. The index finger model consists of four phalanges: distal, middle, proximal, and metacarpal phalanges. These four phalanges are connected by three joints: distal interphalangeal joint (DIP), proximal interphalangeal joint (PIP), and metacarpophalangeal joint (MCP). Figs. 1(a) and (b) illustrate the index finger model at the beginning of motion ($t = 0$) and in touch with the keypad, respectively. The DIP and

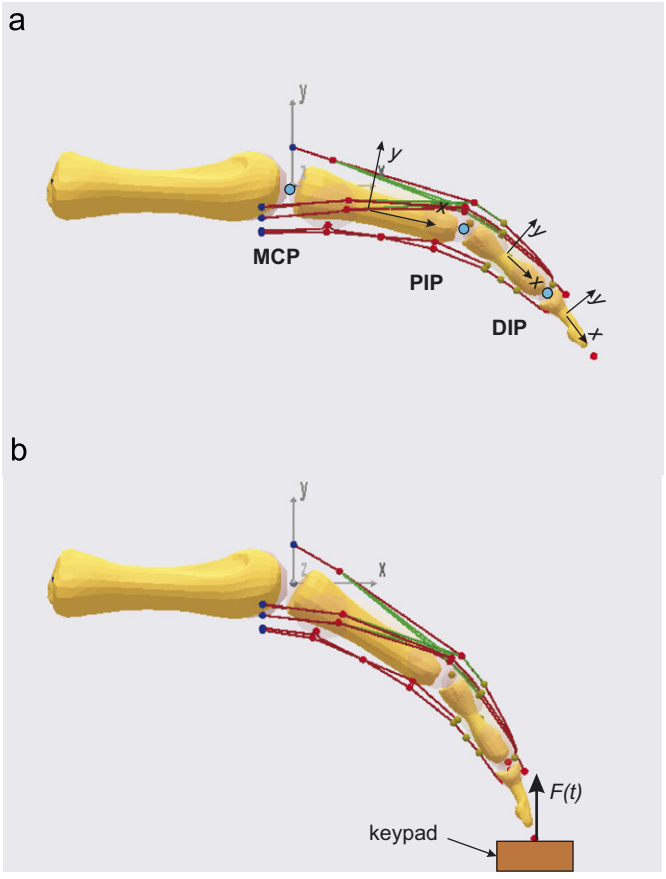

Fig. 1. Index finger model. (a) The index finger model consists of distal, middle, proximal, and metacarpal phalanges, which are linked by DIP, PIP, and MCP joints. (b) The finger is in contact with the keypad during tapping. The interface impact force $F(t)$ is treated as external loading applied on the fingertip.

PIP joints are considered as hinges with one DOF in the z-axis, simulating flexion/extension motion; while the MCP joint is modeled as a universal joint with two DOFs in the y- and z-axes, simulating adduction/abduction and flexion/extension motions, respectively. The dimensional scale of the normative finger model (An et al., 1979) is adopted into the current model. The directions of the coordinate systems of the current model are chosen to be consistent with the normative model. Each phalange has a local coordinate system, located at its mass center. The attachment locations of the tendons are defined according to the normative model (An et al., 1979). Seven muscles were included in the proposed model: flexor digitorum profundus (FP), flexor digitorum superficials (FS), extensor indicis (EI), extensor digitorum communis (EC), radial interosseous (RI), ulnar interosseous (UI), and lumbrical (LU).

2.2. Mass moment of inertia of finger sections

Finger sections are considered to be composed of soft tissue and bone. The bony section contains a canal at the center (Fig. 2). Both soft tissue and bony sections are approximated by cylindrical bodies with ellipsoidal cross sections (Robertson et al., 2004). The mass moments of inertia for each finger section complex are estimated using a superposition technique:

$$I_{xx}(\text{tissue}) = \frac{\pi\rho_t}{4}[(a_t b_t l_t)(a_t^2 + b_t^2) - (a_b b_b l_b)(a_b^2 + b_b^2)],$$

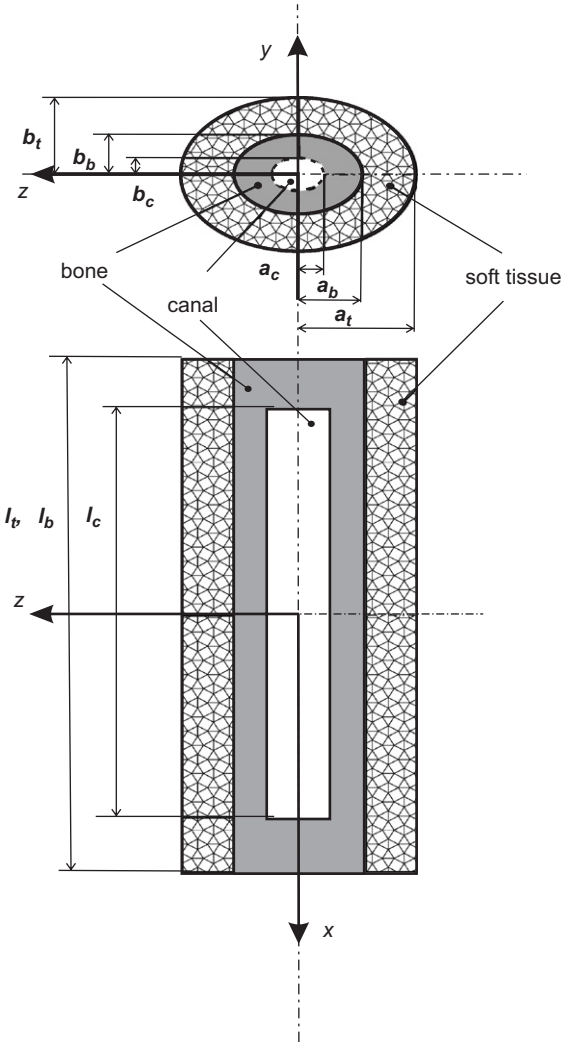

Fig. 2. Finger segments are approximated by cylinders with ellipsoidal cross sections. The finger sections are composed of soft tissue and bone; and the bone has a canal at center.

$$I_{yy}(\text{tissue}) = \frac{\pi\rho_t}{12}[(a_t b_t l_t)(3a_t^2 + l_t^2) - (a_b b_b l_b)(3a_b^2 + l_b^2)],$$

$$I_{zz}(\text{tissue}) = \frac{\pi\rho_t}{12}[(a_t b_t l_t)(3b_t^2 + l_t^2) - (a_b b_b l_b)(3b_b^2 + l_b^2)] \quad (1)$$

and

$$I_{xx}(\text{bone}) = \frac{\pi\rho_b}{4}[(a_b b_b l_b)(a_b^2 + b_b^2) - (a_c b_c l_c)(a_c^2 + b_c^2)],$$

$$I_{yy}(\text{bone}) = \frac{\pi\rho_b}{12}[(a_b b_b l_b)(3a_b^2 + l_b^2) - (a_c b_c l_c)(3a_c^2 + l_c^2)],$$

$$I_{zz}(\text{bone}) = \frac{\pi\rho_b}{12}[(a_b b_b l_b)(3b_b^2 + l_b^2) - (a_c b_c l_c)(3b_c^2 + l_c^2)], \quad (2)$$

where a, b, and l are half width, half depth, and length of the cylinder, respectively; ρ is the mass density; and subscripts, t, b, and c denote soft tissue, bone, and canal, respectively.

The mass moment inertia of the finger section complex is the sum of that of soft tissue and bone. Representative external dimensions of male index finger are adopted from the studies by Garrett (1971) and Buchholz and Armstrong (1991) and listed in Table 1(a). The dimensions of the index finger phalanges are estimated using the measurements by Schulter-Ellis and Lazar (1984) and are also listed in Table 1(a). The mass and the principal mass moment of inertia of each finger section were estimated, as listed in Table 1(b). The reference coordinate of the mass moment of inertia is at the mass center of each finger section (Fig. 2). The relative density of the soft tissues and bone are assumed to be 1.0 and 1.9 (Abe et al., 1996), respectively, in the calculations.

2.3. Muscle model and parameters

All seven muscles of the index finger are modeled using a Hill-type three-element model, i.e., "AnyMuscleModel3E" in AnyBody Simulation System. The three-element muscle model (van den Bogert et al., 1998) consists of a contractile element, an elastic element in parallel with the contractile element, and a serial elastic element, representing the active properties of the muscle fibers, the passive stiffness of the muscle fibers, and the tendon stiffness, respectively. The contractile element contains the force–velocity relationship, isometric force–length relationship, and ratio of fast to slow fibers. The effects of pennation angle and the isometric force–length relationship have been considered in this three-element muscle model (Zajac, 1989).

The maximum isometric muscle force is considered to be proportional to the physiologic cross-section area (PCSA), i.e., $F^{\max} = S \cdot \text{PCSA}$ with $S = 30\,\text{N/cm}^2$ (Epstein and Herzog, 1998). The PCSA and the optimal fiber length of the muscles are adopted from the experimental data reported by Brand and Hollister (1999); and the pennation angle of the muscles is taken from the experimental data by Lieber et al. (1990, 1992) and Jacobson et al. (1992) (Table 2). The ratio of fast to slow muscle fibers is considered to be 1:4 for all muscles.

The recruitment of the muscle forces is calculated by using a min/max optimization procedure in AnyBody (Rasmussen et al., 2001), in which the maximal normalized muscle force is minimized. The cost function of the optimization procedure is

$$\text{Max}(f_i/F_i^{\text{m}}), \quad i = 1, \ldots, N, \quad (3)$$

where f_i and F_i^{m} are the muscle force and the isometric muscle force at optimal length for i muscle, respectively. The minimization of the cost function (Eq. (3)) is subjected to the constraints of $f_i/F_i^{\text{m}} \leqslant 1$ and $f_i \geqslant 0$, with $i = 1, \ldots, N$, and the dynamic force balance. At any instance, the sum of the contributions of each individual muscle to joint moments are calculated and they are balanced with the external forces and the inertial forces of the segments. Physiologically, such an optimization procedure is equivalent to minimizing muscle fatigue (Dul et al., 1984).

2.4. Simulation procedure

The responses of the index finger to tapping are simulated using an inverse dynamic technique. The time histories of the typical impact force

Table 1
Dimensions, mass, and mass moment of inertia of finger sections used in the current study

	Bone external			Bone canal			Tissue external		
(mm)	*a*	*b*	*l*	*a*	*b*	*l*	*a*	*b*	*l*
(a)									
Distal	3.92	2.42	19.67	1.96	0.80	14.75	8.29	6.86	19.67
Middle	5.56	3.48	24.67	2.78	1.15	18.50	9.21	8.11	24.67
Proximal	6.57	4.65	43.57	3.29	1.53	32.68	9.75	9.52	43.57

Finger section	M (kg)	I_{xx} (kg m^2)	I_{yy} (kg m^2)	I_{zz} (kg m^2)
(b)				
Distal	3.91E − 03	1.04E − 07	1.90E − 07	1.70E − 07
Middle	6.79E − 03	2.32E − 07	4.84E − 07	4.51E − 07
Proximal	1.55E − 02	6.48E − 07	2.86E − 06	2.83E − 06

The finger sections consist of soft tissue and bone with a canal, as illustrated in Fig. 2. (a) a, b, and l are the half width, the half depth, and length, respectively. (b) M is mass; I_{xx}, I_{yy}, and I_{zz} are rotational inertias around x-, y-, and z-axis, respectively, and at the mass center of each finger section (Fig. 2). The relative mass densities for soft tissue and bone were considered to be 1.0 and 1.9, respectively, in the calculations.

Table 2
PCSA, fiber length, and pennation angle of the muscles used in the current study

Muscle	PCSA (cm^2)	Fiber length (mm)	Pennation angle (deg)
FP	4.79	66	12.1
FS	4.79	70	3.1
RI	3.53	14	9.2
UI	2.80	15	9.2
LU	0.28	66	1.2
EI	1.12	60	3.5
EC	1.39	60	3.5

at the fingertip (Fig. 3(a)) reported by Jindrich et al. (2004) was applied at the force boundary. The time histories of DIP, PIP, and MCP joint angles during tapping (Figs. 3(b–d)), which are the averaged values of 332 taps collected from 16 subjects, are applied to drive the model. The joint torques and muscle loading are predicted as a function of time. The time histories of DIP, PIP, and MCP joint angles during tapping have been synchronized to that of the fingertip impact force by shifting to the same start of contact and expanding to the contact period. The experimental joint angle data were fitted to fourth-order polynomial curves, which are used as the model inputs. The DIP, PIP, and MCP joint angles for the times immediately before and after the contact period are obtained by extrapolation using the polynomial functions (Figs. 3(b–d)). The time histories of the joint angular velocity and acceleration are plotted in Figs. 3(e) and (f), respectively. These curves were obtained by differentiations of the time histories of the joint angles.

Before the inverse dynamic calculations, the tendon lengths of the model are adjusted to minimize the passive muscle force. The passive muscle forces of the model are minimized at the initial posture of the finger. The simulations are performed in two stages: (a) Calculation of the joint torques in response to the prescribed joint motions. In this stage, all three joints are constrained and the joint reactions are considered as the joint torques. (b) Calculation of the muscle loading. The constraints in the joints are removed, and the joint torques are carried by the muscles in this stage.

3. Results

The time histories of torque in DIP, PIP, and MCP joints during tapping are predicted and compared with the results by Jindrich et al. (2004), as shown in Figs. 4(a), (c), and (e), respectively. The torque in the DIP joint predicted using our model is approximately 18% less than that by Jindrich et al. (2004), while the predicted torques in the PIP and MCP joints agree well with the previous results (with relative difference less than 9%). The patterns of the relationships of joint torque and joint angle obtained in the current study agree well with those reported by Jindrich et al. (2004) (Figs. 4(b), (d), and (f)).

The time histories of the active force (F_m), passive force (F_p), and total force (F_t) of all seven muscles are depicted (Figs. 5(a–g)) and compared qualitatively with the EMG data measured by Kuo et al. (2006) (Fig. 5(h)), which are related to the muscle activation timing. LUM, FDI, FDS, FDP, and EDC in Fig. 5(h) are corresponding to the LU, UI/RI, FS, FD, and EI/EC muscle, respectively, in the current study. The fingertip/keypad contact period for Kuo et al.'s (2006) study is approximately 90 ms, while that for the current simulations are approximately 180 ms. Despite the difference of the contact period for these two different studies, the time sequences of the muscle activations predicted in the current study are comparable with those of the EMG measurements. The model predictions indicate that the EI and EC muscles, which correspond to the EDC in EMG studies, are activated before the initiation of the downswing motion; shortly before contact, FS, FP, UI, and RI muscles, which correspond to FDS, FDP, and FDI in EMG studies, are activated; and finally EI and EC muscles are re-activated. The only muscle for which the model predictions are not in complete agreement with the EMG signal is the LU muscle.

A close examination of the predicted muscle forces revealed that the maximum passive forces occurred in UI and RI muscles, which represent approximately 18% and 10% of the total force at peak, respectively (Fig. 5). The passive forces in all other muscles are negligible, and they represent less than 5% of the total muscle force at peak during the entire tapping period. The major

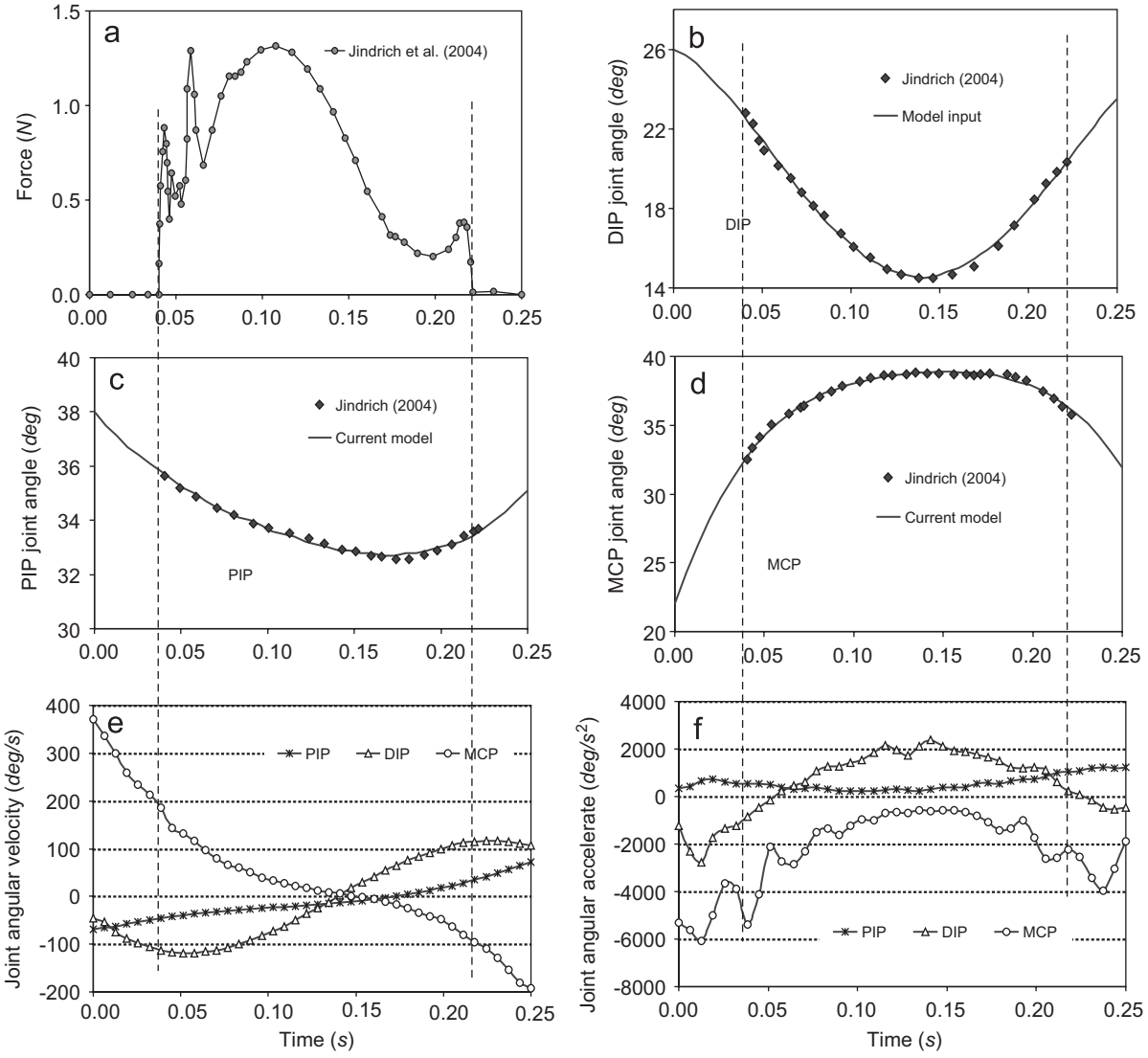

Fig. 3. Time histories of representative force at fingertip and joint angles of an index finger during keypad strike reported by the previous researchers (Jindrich et al., 2004). (a) impact force at the fingertip; (b) DIP joint angle; (c) PIP joint angle; (d) MCP joint angle; (e) joint angular velocity; (f) joint angular accelerate. The first dashed line represents the start of the contact and the second dashed line represents the end of the contact. The experimental measurements shown in (a)–(d) have been used as model input in the current study.

muscle forces occurred during the impact period in FP, FS, UI, and RI muscles, while they occurred before and after the impact in EI and EC muscles. The muscle force in the LU muscle is very small compared with that of other muscles.

4. Discussion and conclusion

It has been hypothesized that MSDs of the upper extremities seen in computer users are associated with repetitive excessive muscle force production in the hands. Thus, understanding time-dependent muscle forces during key tapping is essential for bioengineers and ergonomic designers to optimize keyboard design and minimize hand injuries in the operators. In the current study, we theoretically predicted the time histories of the joint torques and muscle forces in an index finger during tapping. Since the proposed model can include realistic bony shapes, nonlinear mechanical properties of the ligaments and tendons, and physiological muscle models, and, most important, it has been developed on a platform of the commercial software package AnyBody, our results and approach can be used to solve practical problems by bioengineers and ergonomic designers.

It has been well recognized that muscle tension will lag behind the EMG signal under dynamic contraction (e.g., Winter, 2005). The delay of the muscle force is due to the fact that the twitch corresponding to each motor unit activation potential reaches its peak 40–100 ms afterward. Thus, the resulting summation of twitch forces will have a delay behind the EMG signals. A comparison of the timing of the predicted muscle forces with the corresponding

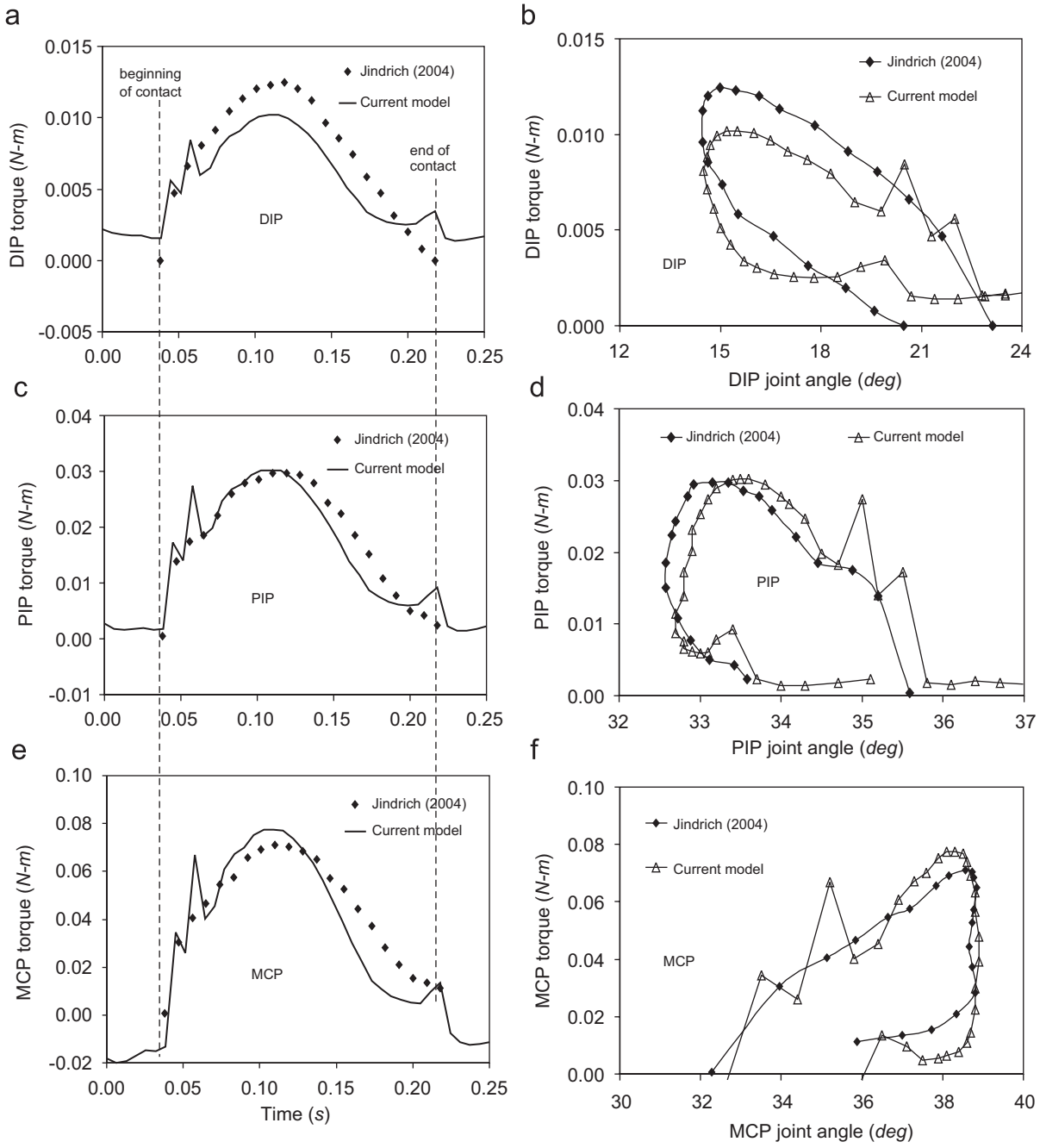

Fig. 4. Comparison of the predicted time histories of the joint torques (left column) and the joint torque/angle relationships (right column) with those reported by Jindrich et al. (2004). (a) and (b) DIP joint, (c) and (d) PIP joint, and (e) and (f) MCP joint.

EMG data indicated that the predicted muscle forces lag consistently behind the EMG signals by approximately 100 ms, which is reasonable compared with the previous studies (e.g., Crosby, 1978).

The comparison of the predicted time histories of muscle forces with the EMG signals (Kuo et al., 2006) indicated that the time sequences of the predicted forces of FP, FS, UI, RI, EI, and EC muscles are consistent with the time sequences of the corresponding EMG signals, while that of LU muscle is not (Fig. 5). The model predictions indicate that the maximal force magnitude in the LU muscle is negligible compared with those of the other muscles, while the EMG data showed that it was activated before the downswing period. An activated muscle could carry a small force that does not make a significant contribution in comparison to other activated muscles. Therefore, the model predictions for the LU muscle actually are not inconsistent with the EMG data.

The predicted maximal peak forces in FS and FP tendons (1.24 and 3.80 N, as shown in Figs. 5(a) and (b), respectively) reach approximately 0.95 and 2.90 times, respectively, of the maximal force at the fingertip (1.31 N,

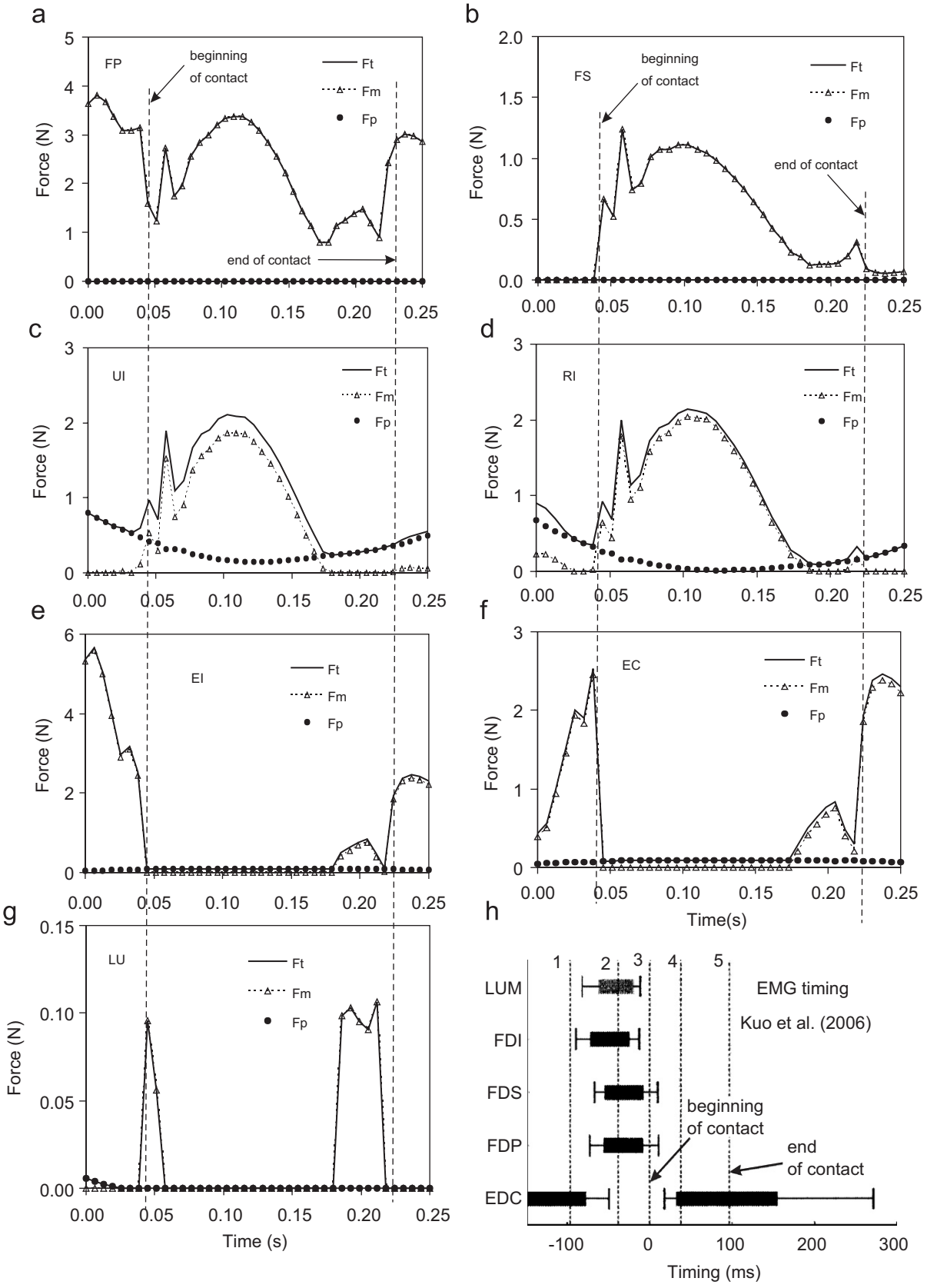

Fig. 5. Predicted muscle forces in an index finger during tapping are compared with EMG measurements reported by Kuo et al. (2006). F_m, F_p, and F_t are active, passive, and total muscle force, respectively. (a) FP, (b) FS, (c) UI, (d) RI, (e) EI, (f) EC, (g) LU, (h) EMG measurements reported by Kuo et al. (2006). LUM, FDI, FDS, FDP, and EDC of the EMG measurements in (h) (Kuo et al., 2006) are corresponding to the LU, UI/RI, FS, FD, and EI/EC muscle, respectively, in the current study. The figures show that the time sequences of the forces of FP, FS, UI, RI, EI, and EC muscles are consistent with the time sequences of the corresponding EMG signals, while that of LU muscle does not.

as shown in Fig. 3(a)). Our model predictions are consistent with the recent experimental data reported by Kursa et al. (2005), but they are substantially smaller than the early experimental data reported by Schuind et al. (1992) and Dennerlein et al. (1999).

The effects of the external force and mass moment of inertia on the muscle force could be roughly evaluated by a comparison of the muscle forces (Fig. 5) with contact force (Fig. 3(a)) and joint angular velocity and acceleration (Figs. 4(e) and (f)). The first peak observed in the time histories of the muscle force should be related to the effects of the mass moment of inertia of the finger sections because it occurred around 25–30 ms, before the fingertip and keypad came into contact and when the joint accelerations reach their peak. The second and third peaks were observed in the time histories of FP, FS, UI, and RI muscle forces, and occurred around 50 and 110 ms, respectively. These two peaks are likely related to external forces applied at the fingertip, which also reach their maximums around those times (Fig. 3(a)).

The slight differences in the predicted joint torques between the current study and those by Jindrich et al. (2004) (Fig. 4) might be explained by the differences in finger section lengths and impact forces. It should be noted that the results reported by Jindrich et al. (2004) are the averages from 332 taps by 15 subjects. In the current simulations, the time histories of a typical impact force and the averaged joint angles were used as model inputs. Considering the differences in finger section lengths and experiments in each trial, these differences in the joint torques are in a reasonable range.

In the current model, the damping effects of the soft tissues are not considered. Consequently, the joint torques and muscle forces at peaks predicted in our simulations may be greater than what actually happens under physiological conditions.

A further limitation of the current study is that the simulations were performed using the experimental data reported by Jindrich et al. (2004), while the predicted muscle forces were compared with the EMG signals reported by Kuo et al. (2006). The period of the contact between the fingertip and keypad in the study by Jindrich et al. (2004) is about twice as long as that by Kuo et al. (2006). The difference in contact periods of two different studies made the comparison of the model predictions with the EMG measurements be limited only in time sequence and qualitative in nature.

In summary, we have theoretically analyzed the muscle forces and joint torques in an index finger during a tapping task in the current study. Our results suggested that the muscle forces in the finger during tapping are mainly related to the impact force at the fingertip. The proposed model can be used by researchers to improve the design for keypads and posture to minimize the impact force at the fingertip, thereby reducing the musculoskeletal loading of the hand and operators' fatigue and injury risk.

Disclaimers

The findings and conclusions in this report are those of the authors and do not necessarily represent the views of the National Institute for Occupational Safety and Health.

Conflict of interest

All authors of this manuscript have no conflict of interest.

References

Abe, H., Hayashi, K., Sato, M., 1996. Mechanical Properties of Living Cells, Tissues, and Organs. Springer, Tokyo.

An, K.N., Chao, E.Y., Cooney, W.P., Linscheid, R.L., 1979. Normative model of human hand for biomechanical analysis. Journal of Biomechanics 12 (10), 775–788.

Biggs, J., Horch, K., 1999. A three-dimensional kinematic model of the human long finger and the muscles that actuate it. Medical Engineering and Physics 21 (9), 625–639.

Brand, P.W., Hollister, A.M., 1999. Clinical Mechanics of the Hand, third ed. Mosby, Inc., St. Louis, Baltimore, Boston.

Brook, N., Mizrahi, J., Shoham, M., Dayan, J., 1995. A biomechanical model of index finger dynamics. Medical Engineering and Physics 17 (1), 54–63.

Buchholz, B., Armstrong, T.J., 1991. An ellipsoidal representation of human hand anthropometry. Human Factors 33 (4), 429–441.

Cail, F., Aptel, M., 2003. Biomechanical stresses in computer-aided design and in data entry. International Journal of Occupational Safety and Ergonomics 9 (3), 235–255.

Crosby, P.A., 1978. Use of surface electromyography as a measure of dynamic force in human limb muscles. Medical and Biological Engineering and Computing 16, 519–524.

Day, J.C., Janus, A., Davis, J., 2005. Computer and internet use in the United States: 2003. U.S. Census Bureau. Current Population Reports. Special Studies. U.S. Department of Commerce.

Dennerlein, J.T., Diao, E., Mote Jr., C.D., Rempel, D.M., 1998. Tensions of the flexor digitorum superficialis are higher than a current model predicts. Journal of Biomechanics 31 (4), 295–301.

Dennerlein, J.T., Diao, E., Mote Jr., C.D., Rempel, D.M., 1999. In vivo finger flexor tendon force while tapping on a keyswitch. Journal of Orthopaedic Research 17 (2), 178–184.

Dul, J., Johnson, G.E., Shiavi, R., Townsend, M.A., 1984. Muscular synergism—ii. A minimum-fatigue criterion for load sharing between synergistic muscles. Journal of Biomechanics 17 (9), 675–684.

Epstein, M., Herzog, W., 1998. Theoretical Models of Skeletal Muscle, first ed. Wiley, Chichester, New York, Weinheim, Brisbance, Singapore, Toronto.

Faucett, J., Rempel, D., 1996. Musculoskeletal symptoms related to video display terminal use: an analysis of objective and subjective exposure estimates. AAOHN Journal 44 (1), 33–39.

Garrett, J.W., 1971. The adult human hand: some anthropometric and biomechanical considerations. Human Factors 13 (2), 117–131.

Gerard, M.J., Armstrong, T.J., Franzblau, A., Martin, B.J., Rempel, D.M., 1999. The effects of keyswitch stiffness on typing force, finger electromyography, and subjective discomfort. American Industrial Hygiene Association Journal 60 (6), 762–769.

Gerr, F., Monteilh, C.P., Marcus, M., 2006. Keyboard use and musculoskeletal outcomes among computer users. Journal of Occupational Rehabilitation 16 (3), 265–277.

Hales, T.R., Sauter, S.L., Peterson, M.R., Fine, L.J., Putz-Anderson, V., Schleifer, L.R., Ochs, T.T., Bernard, B.P., 1994. Musculoskeletal disorders among visual display terminal users in a telecommunications company. Ergonomics 37 (10), 1603–1621.

Jacobson, M.D., Raab, R., Fazeli, B.M., Abrams, R.A., Botte, M.J., Lieber, R.L., 1992. Architectural design of the human intrinsic hand muscles. Journal of Hand Surgery [American Volume] 17 (5), 804–809.

Jindrich, D.L., Balakrishnan, A.D., Dennerlein, J.T., 2004. Finger joint impedance during tapping on a computer keyswitch. Journal of Biomechanics 37 (10), 1589–1596.

Kuo, P.L., Lee, D.L., Jindrich, D.L., Dennerlein, J.T., 2006. Finger joint coordination during tapping. Journal of Biomechanics 39 (16), 2934–2942.

Kursa, K., Diao, E., Lattanza, L., Rempel, D., 2005. In vivo forces generated by finger flexor muscles do not depend on the rate of fingertip loading during an isometric task. Journal of Biomechanics 38 (11), 2288–2293.

Lieber, R.L., Fazeli, B.M., Botte, M.J., 1990. Architecture of selected wrist flexor and extensor muscles. Journal of Hand Surgery [American Volume] 15 (2), 244–250.

Lieber, R.L., Jacobson, M.D., Fazeli, B.M., Abrams, R.A., Botte, M.J., 1992. Architecture of selected muscles of the arm and forearm: anatomy and implications for tendon transfer. Journal of Hand Surgery [American Volume] 17 (5), 787–798.

Marcus, M., Gerr, F., 1996. Upper extremity musculoskeletal symptoms among female office workers: associations with video display terminal use and occupational psychosocial stressors. American Journal of Industrial Medicine 29 (2), 161–170.

Nelson, J.E., Treaster, D.E., Marras, W.S., 2000. Finger motion, wrist motion and tendon travel as a function of keyboard angles. Clinical Biomechanics (Bristol Avon) 15 (7), 489–498.

Rasmussen, J., Damsgaard, M., Voigt, M., 2001. Muscle recruitment by the min/max criterion—a comparative numerical study. Journal of Biomechanics 34 (3), 409–415.

Robertson, D.G., Hamill, J., Kamen, G., Caldwell, G.E., Whittlesey, S., 2004. Research Methods in Biomechanics. Human Kinetics Publishers.

Sancho-Bru, J.L., Perez-Gonzalez, A., Vergara-Monedero, M., Giurintano, D., 2001. A 3-d dynamic model of human finger for studying free movements. Journal of Biomechanics 34 (11), 1491–1500.

Sancho-Bru, J.L., Perez-Gonzalez, A., Vergara, M., Giurintano, D.J., 2003. A 3d biomechanical model of the hand for power grip. Journal of Biomechanical Engineering 125 (1), 78–83.

Schuind, F., Garcia-Elias, M., Cooney III, W.P., An, K.N., 1992. Flexor tendon forces: in vivo measurements. Journal of Hand Surgery [American Volume] 17 (2), 291–298.

Schulter-Ellis, F.P., Lazar, G.T., 1984. Internal morphology of human phalanges. Journal of Hand Surgery [American Volume] 9 (4), 490–495.

Valero-Cuevas, F.J., 2005. An integrative approach to the biomechanical function and neuromuscular control of the fingers. Journal of Biomechanics 38 (4), 673–684.

Valero-Cuevas, F.J., Johanson, M.E., Towles, J.D., 2003. Towards a realistic biomechanical model of the thumb: the choice of kinematic description may be more critical than the solution method or the variability/uncertainty of musculoskeletal parameters. Journal of Biomechanics 36 (7), 1019–1030.

van den Bogert, A.J., Gerritsen, K.G., Cole, G.K., 1998. Human muscle modelling from a user's perspective. Journal of Electromyography and Kinesiology 8 (2), 119–124.

Winter, D.A., 2005. Biomechanics and Motor Control of Human Movement, third ed. Wiley, Hoboken, NJ.

Woods, M., Babski-Reeves, K., 2005. Effects of negatively sloped keyboard wedges on risk factors for upper extremity work-related musculoskeletal disorders and user performance. Ergonomics 48 (15), 1793–1808.

Zajac, F.E., 1989. Muscle and tendon: properties, models, scaling, and application to biomechanics and motor control. Critical Reviews in Biomedical Engineering 17 (4), 359–411.